

## Wear performance of in-situ aluminum matrix composite after micro-arc oxidation

Yaman ERARSLAN

Department of Metallurgical and Materials Engineering, Faculty of Chemical and Metallurgical Engineering,  
Yildiz Technical University, Davutpasa Campus, 34210 Esenler, Istanbul, Turkey

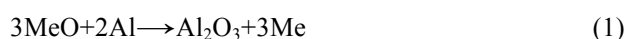
Received 7 March 2012; accepted 11 October 2012

**Abstract:** An attempt was made to modify the surface of in-situ aluminium matrix composite (AMC) by micro-arc oxidation (MAO). In the microstructure of AMC,  $\text{CuAl}_2$  reinforcements were generated by introducing 15% CuO into the aluminium melt. AMC was hot forged, homogenised, quenched and artificially aged before the MAO in a KOH, KF and  $\text{Na}_2\text{SiO}_3$ -containing electrolyte. After the MAO process the surface of the AMC was covered with  $\text{Al}_2\text{O}_3$  coating having an effective thickness of about 15  $\mu\text{m}$ . Appearance of crack and/or delamination free zones at the periphery of the indent after the Rockwell C adhesion test indicated good adhesion between the composite and the  $\text{Al}_2\text{O}_3$  coating. During dry sliding wear tests, this adherent  $\text{Al}_2\text{O}_3$  coating resisted the destructive action of the  $\text{Al}_2\text{O}_3$  ball and provided about 15 times enhancement in wear resistance as compared to the original state.

**Key words:** in situ composite; aluminum matrix composite; microarc oxidation; wear; tribology

### 1 Introduction

The aluminum matrix composites (AMCs) are conventionally produced by introducing ceramic based hard particles such as oxides, carbides and borides into the aluminum melt. Since these reinforcing particles were added into the aluminum melt externally, this conventional composite production method goes by the name of ex-situ. The main disadvantages of ex-situ composite production are the weak interfacial bonding between the reinforcing particle and the matrix and inhomogeneous distribution of the reinforcements in the microstructure [1–6]. In order to eliminate these problems, in-situ composite production method, which bases on the natural formation of the reinforcing particles during solidification, has been developed [7–12]. In general, in-situ AMCs are produced by adding metal oxides (MeO) into the aluminum melt to induce  $\text{Al}_2\text{O}_3$  precipitation according to the following reaction [12]:



Although AMCs have come into use increasingly in many engineering applications, it is further required from these composites to provide much better wear resistance without damage and/or detachment of the reinforcement

particles [13–24]. From the tribological point of view, this goal can be achieved by covering the surfaces with hard coatings. Among the surface modification techniques, MAO process, which leads the development of hard ceramic coatings on many light metals such as Al, Ti, and Mg, appeared as a very attractive processing in recent years [24–34]. In the literature, there are many reports declaring the enhancement of wear resistance of monolithic aluminium alloys after MAO as a result of covering of the surface with  $\text{Al}_2\text{O}_3$  coating [35–40]. However there are few publications on the contribution of MAO process on the tribological performance of ex-situ AMC's such as  $\text{Al383/SiO}_2$ ,  $\text{Al356/SiC}$  [41–46]. To the author's knowledge, MAO of in-situ AMCs has not been studied yet. This study was initiated to modify the surfaces of an in-situ AMC via MAO with the aim to enhance the resistance against the destructive action of the counterfaces under sliding contact conditions.

### 2 Experimental

Commercially pure aluminum (purity 99.1%) and CuO powders having an average particle size of 40  $\mu\text{m}$  were used as the starting materials. First of all, the aluminum was melted in SiC crucible and kept at 750 °C

for 15 min in argon atmosphere. Compacted CuO powders, which were wrapped into aluminum foils, were added into the melt at mass fraction of 15% after holding the compacts at 200 °C for 2 h. Then, the melt was mixed for 3–4 min in order to enable CuO to distribute homogeneously. Finally, the mixture was poured into the mold having dimensions of 60 mm×60 mm×120 mm. After solidification the samples were homogenized at 500 °C for 6 h and then rolled at 400 °C with reduction rate of 50%. The hot deformed samples were then aged at 190 °C for 12 h after solutionizing at 495 °C. The hardness of the aged sample was measured as HV<sub>10</sub> 145.

The samples, which were prepared from the aged composite with dimensions of 30 mm×30 mm×5 mm, were subjected to MAO process in an electrolyte containing KOH, KF and Na<sub>2</sub>SiO<sub>3</sub>. MAO was conducted at positive and negative constant voltage modes of 500 V and 83 V, respectively, for 5 min.

The structural characterization of the samples was conducted on an energy diffraction spectroscopy (EDS) equipped scanning electron microscope (SEM, JEOL 5410 LV) and X-ray diffractometer (XRD, GBC X-Ray EQ.) SEM examinations were made after etching the polished samples with Keller's reagent. XRD analyses were conducted at 5° and 90° in 2θ interval by using Cu K<sub>α</sub> radiation.

The adherence between the coating and the AMC was evaluated by penetrating the conic Rockwell C indenter under a load of 1470 N (Rockwell C adhesion test). Wear tests were made on a low frequency reciprocating Tribotechnic tribometer, by rubbing 6 mm-diameter Al<sub>2</sub>O<sub>3</sub> ball on the surface of the samples under the normal load of 2 N. The sliding velocity and total sliding distance were 10 mm/s and 25 m, respectively. Wear tests were conducted at temperature of 20 °C and relative humidity of 35 % under dry sliding conditions. After the wear test, the wear tracks formed on the coatings were detected by a 2D surface profilometer (MahrPerhen S&P Perthometer) and a SEM. The contact surface of the Al<sub>2</sub>O<sub>3</sub> ball was also examined by an optical microscope. It should be noted that for the Rockwell C adhesion and wear tests the surfaces of the samples were ground and polished gently after MAO process.

### 3 Results and discussion

The XRD pattern and SEM micrograph of the aged composite (hereafter will be referred as original composite) are depicted in Figs. 1 and 2. On the XRD pattern (Fig. 1) of the original composite only the peaks of aluminum and CuAl<sub>2</sub> were clearly detected. It is therefore suggested that the metallic copper formed as the result of the following reaction:



exceeded the dissolution limit of copper in aluminum and led to the precipitation of CuAl<sub>2</sub>, as also reported by HOSEINI and MERATIAN [12]. Disappearance of Al<sub>2</sub>O<sub>3</sub> peaks on the XRD pattern (Fig. 1) can be attributed to its low volume fraction. In accordance with the result of XRD studies, EDS equipped SEM surveys (Fig. 2 and Table 1) confirmed the precipitation of CuAl<sub>2</sub> (bright colored regions in Fig. 2) in the aluminum matrix (dark colored regions in Fig. 2).

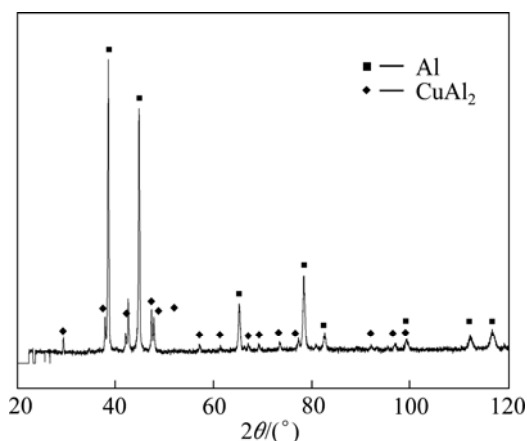


Fig. 1 XRD pattern of examined composite

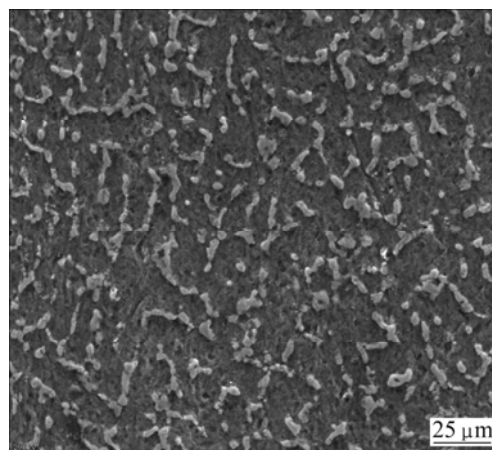


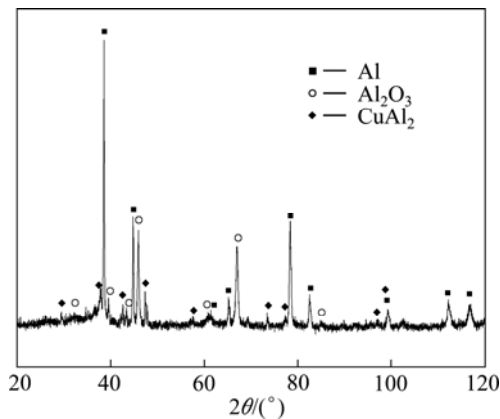
Fig. 2 SEM micrograph of examined composite

Table 1 EDS analysis results of matrix (dark coloured regions) and precipitates (white coloured regions)

Element	Composition/%	
	Matrix	Precipitate
O	98.4	0.6
Al	1.6	70.2
Cu	—	29.2

The XRD pattern of the composite after the MAO process is given in Fig. 3. On the XRD pattern, in addition to the peaks of aluminum and CuAl<sub>2</sub>, which also

present in the XRD pattern of the original composite (Fig. 1), the peaks of  $\text{Al}_2\text{O}_3$  also appeared. This observation indicated that the surfaces of the composite were covered with  $\text{Al}_2\text{O}_3$  coating, similar to the monolithic aluminum alloys [40–45] and ex-situ AMCs [46–52] after the MAO process.

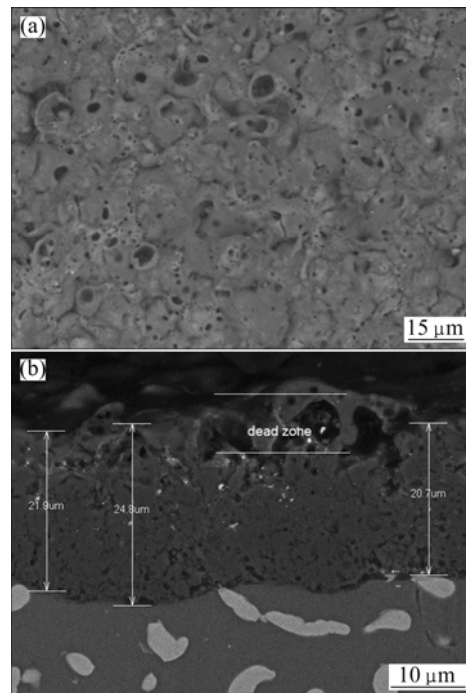


**Fig. 3** XRD pattern of examined composite after MAO process

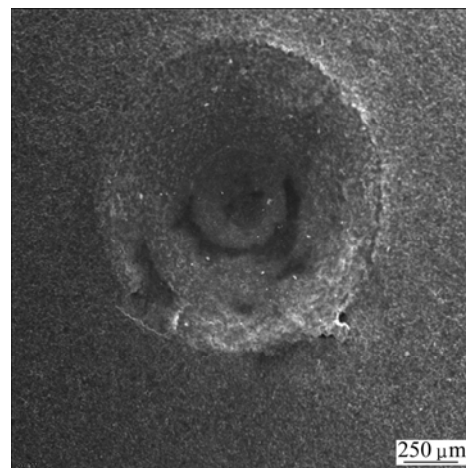
The surface and cross-section SEM micrographs of the MAO coated composite are presented in Fig. 4. Surface examinations revealed that  $\text{Al}_2\text{O}_3$  coating was very rough and porous (Fig. 4(a)). Cross-section examinations showed that the coarse pores were mostly located at the outermost section of the  $\text{Al}_2\text{O}_3$  coating (Fig. 4(b)), which is generally named as the dead zone. The average thicknesses of the coating were measured to be about 22  $\mu\text{m}$ . If the dead zone, which had a thickness of about 7  $\mu\text{m}$ , was excluded the effective thickness of the coating reduced to about 15  $\mu\text{m}$ . It should finally be mentioned that no detachment at the interfaces of aluminum matrix/ $\text{Al}_2\text{O}_3$  coating and/or  $\text{CuAl}_2$  precipitate/ $\text{Al}_2\text{O}_3$  coating was detected by SEM examination. As mentioned in the experimental section, the dead zone of the  $\text{Al}_2\text{O}_3$  coatings was removed before the Rockwell C adhesion and wear tests.

Figure 5 shows the indent formed on the  $\text{Al}_2\text{O}_3$  coating after the Rockwell C adhesion test. Since no evidence of delimitation and cracking was detected at the periphery of the indent, it was concluded that good adherence had been achieved between the  $\text{Al}_2\text{O}_3$  coating and the substrate.

The results of wear tests conducted on the original and MAO coated composites are presented in Figs. 6–9. Wider and deeper wear tracks were developed on the surfaces of the original composite as compared to the MAO coated composites (Fig. 6). By considering the average cross sectional areas of the wear tracks, the enhancement in the wear resistance of the composite after the MAO process was quantified as 15 times. When the contact surface of the original composite/ $\text{Al}_2\text{O}_3$  ball tribo-couple was inspected, it was seen that the original



**Fig. 4** SEM micrographs of surface (a) and cross-section (b) of composite after MAO process



**Fig. 5** SEM micrograph showing periphery of indent after Rockwell C adhesion test conducted after MAO process

composite encountered heavy material loss as the result of the excessive deformation and delimitation. The wear products were adhered on the contact surface of the  $\text{Al}_2\text{O}_3$  ball (Fig. 8). On the MAO coated composite, the depths of the wear tracks were well below the thickness of the  $\text{Al}_2\text{O}_3$  coating. Thus, wear progressed on the  $\text{Al}_2\text{O}_3$  coating and the rubbing action of the  $\text{Al}_2\text{O}_3$  ball caused smoothening of the  $\text{Al}_2\text{O}_3$  coating without any evidence of local delamination. In this respect, material transfer from  $\text{Al}_2\text{O}_3$  coating to the contact surface of the  $\text{Al}_2\text{O}_3$  ball was not identified. When the friction curves were concerned, MAO coated surface led to higher friction coefficient than the original composite (Fig. 9). This

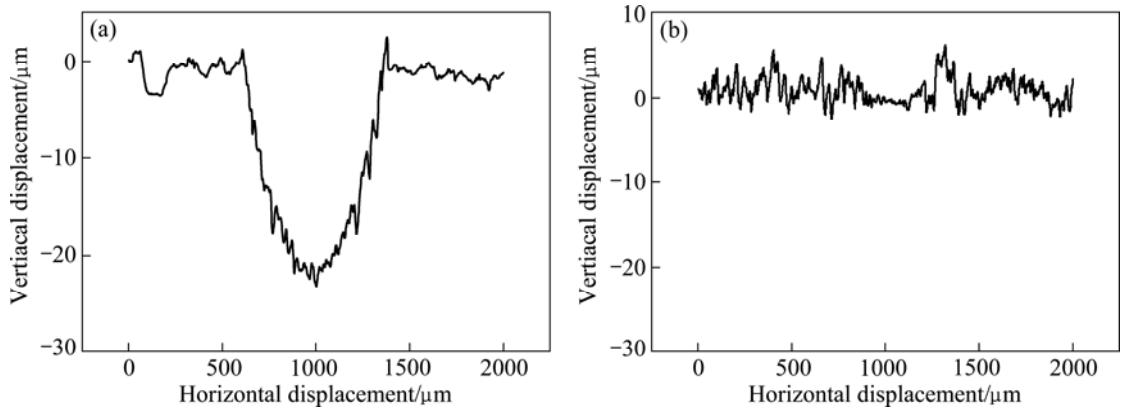


**Fig. 6** Wear tracks profiles formed on surface of composite: (a) Original; (b) MAO coated

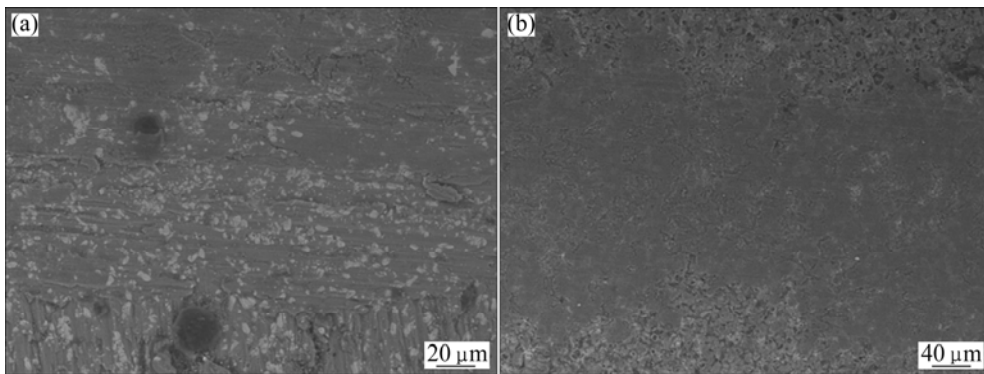


**Fig. 7** SEM micrographs of contact surfaces of composites: (a) Original; (b) MAO coated

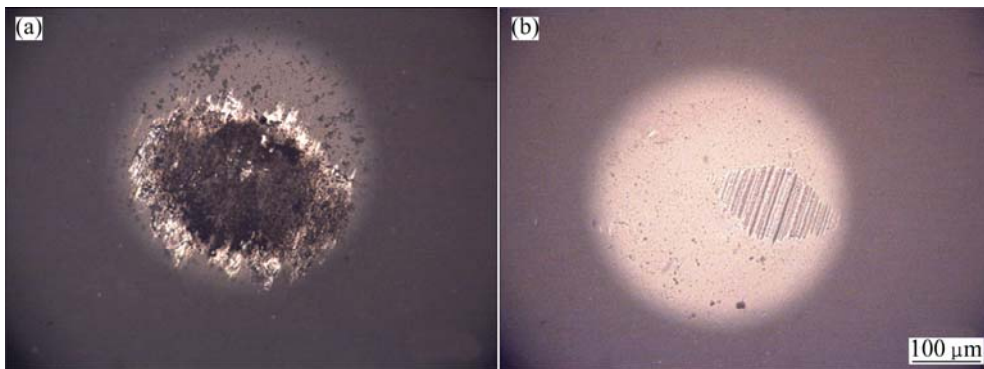


**Fig. 8** Optical micrographs of contact surfaces of Al<sub>2</sub>O<sub>3</sub> balls: (a) Original; (b) MAO coated

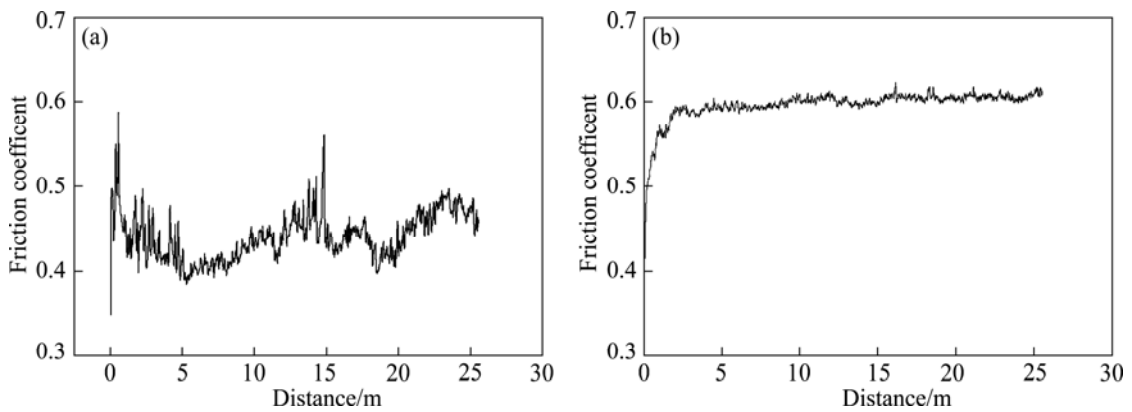


**Fig. 9** Friction curves of examined materials: (a) Original; (b) MAO coated

suggested the crucial role of the wear particles at the interface between the  $\text{Al}_2\text{O}_3$  ball and the bare composite, which also induced a large scatter on the friction curve throughout the testing period. In the case of MAO coated sample, where any material transfer was detected from the  $\text{Al}_2\text{O}_3$  coating to the contact surface of the  $\text{Al}_2\text{O}_3$  ball, the friction coefficient was very smooth.

## 4 Conclusions

1) MAO process was successfully applied to an in-situ  $\text{CuAl}_2$  reinforced AMC by covering the surfaces with an adherent  $\text{Al}_2\text{O}_3$  coating having an effective thickness of about 15  $\mu\text{m}$ . No evidence of delamination and cracking was detected at the periphery of the indent after the Rockwell C adhesion test was conducted on the  $\text{Al}_2\text{O}_3$  coating.

2) This  $\text{Al}_2\text{O}_3$  coating effectively protected the substrate against the destructive action of the  $\text{Al}_2\text{O}_3$  ball during dry sliding wear testing. As compared to the original state, MAO provided about 15 times enhancement in wear resistance of the examined AMC.

## Acknowledgement

The author highly appreciates the contribution of Prof. H. CIMENOGLU to this study.

## References

- [1] IBRAHIM A, MOHAMED F A, LAVERNIA E J. Particulate reinforced metal matrix composites—A review [J]. *Journal of Materials Science*, 1991, 26: 1137–1156.
- [2] ROHATGI K, RAY S, ASTHANA R, NARENDRANATH C S. Interfaces in cast metal-matrix composites [J]. *Materials Science and Engineering A*, 1993, 162(1–2): 163–174.
- [3] LLOYD D J. Particle reinforced aluminum and magnesium matrix composites [J]. *International Materials Reviews*, 1994, 39(1): 1–23.
- [4] FEEST E A. Interfacial phenomena in metal-matrix composites [J]. *Composites*, 1994, 25(2): 75–86.
- [5] HASHIM J, LOONEY L, HASHMI M S J. Particle distribution in cast metal matrix composites—Part I [J]. *Journal of Materials Processing Technology*, 2002, 123(2): 251–257.
- [6] MIRACLE D B. Metal matrix composites from science to technological significance [J]. *Composites Science and Technology*, 2005, 65(15–16): 2526–2540.
- [7] MAITY P C, PANIGRAHI S. C, CHAKRABOTY P N. Preparation of Al– $\text{MgAl}_2\text{O}_4$ – $\text{MgO}$  in situ particle-composites by addition of  $\text{MnO}_2$  particles to molten Al–2 wt% Mg alloys [J]. *Materials Letters*, 1994, 20(3–4): 93–97.
- [8] MAITY P C, CHAKRABOTY P N, PANIGRAHI S C. Al– $\text{Al}_2\text{O}_3$  in situ particle composites by reaction of CuO particles in molten pure Al [J]. *Materials Letters*, 1997, 30(2–3): 147–151.
- [9] ZHANG X P, YE L, MAI Y W, QUAN G F, WEI W. Investigation on diffusion bonding characteristics of SiC particulate reinforced aluminium metal matrix composites (Al/SiC<sub>p</sub>–MMC) [J]. *Composites Part A*, 1999, 30(12): 1415–1421.
- [10] TJONG S C, MA Z Y. Microstructural and mechanical characteristics of in situ metal matrix composites [J]. *Materials Science Engineering R*, 2000, 29: 49–113.
- [11] FAN T, ZHANG D, YANG G, SHIBAYANAGI T, NAKA M. Fabrication of in situ  $\text{Al}_2\text{O}_3/\text{Al}$  composite via remelting [J]. *Journal of Materials Processing Technology*, 2003, 142(2): 556–561.
- [12] HOSEINIA M, MERATIAN M. Fabrication of in situ aluminum–alumina composite with glass powder [J]. *Journal of Alloys and Compounds*, 2009, 471(1–2): 378–382.
- [13] HOSKING F M, PORTILLO F F, WUNDERLIN R, MEHRABIAN R. Composite of Al alloys: Fabrication and wear behavior [J]. *Journal of Materials Science*, 1982, 17(2): 477–498.
- [14] SURAPPA M K, PRASAD S V, ROHATGI P K. Wear and abrasion of cast Al–alumina particle composites [J]. *Wear*, 1982, 77(3): 295–302.
- [15] ALPAS A T, ZHANG J. Wear rate transitions in cast Al–Si alloys reinforced with SiC particles [J]. *Scripta Metallurgica et Materialia*, 1992, 26(3): 505–509.
- [16] MODÍ O P, PRASAD B K, YEGNESWARAN A H, VAIDYA M L. Dry sliding wear behaviour of squeeze cast aluminum alloy–silicon carbide composites [J]. *Materials Science and Engineering A*, 1992, 151(2): 235–245.
- [17] ZHANG J, ALPAS A T. Wear regimes and transitions in  $\text{Al}_2\text{O}_3$  particulate-reinforced Al alloys [J]. *Materials Science and Engineering A*, 1993, 161(2): 273–284.
- [18] MOUSTAFA S F. Wear and wear mechanisms of Al–22% Si/ $\text{Al}_2\text{O}_3$  composite [J]. *Wear*, 1995, 185(1): 189–195.
- [19] SHEU C Y, LIN S J. Particle size effects on the abrasive wear of 20 vol% SiC<sub>p</sub>/7075Al composites [J]. *Scripta Materialia*, 1996, 35(11): 1271–1276.
- [20] WILSON S, ALPAS A T. Wear mechanism map for metal matrix composites [J]. *Wear*, 1997, 212(1): 41–49.
- [21] YANG L J. The effect of nominal specimen contact area on the wear coefficient of A6061 aluminium matrix composite reinforced with alumina particles [J]. *Wear*, 2007, 263(7–12): 939–948.
- [22] STRAFFELINI G, BONOLLOF, MOLINARI A, TIZIANI A. Influence of matrix hardness on the dry sliding behaviour of 20 vol%  $\text{Al}_2\text{O}_3$ -particulate-reinforced 6061 Al metal matrix composite [J]. *Wear*, 1997, 211(2): 192–197.
- [23] ZHANG Peng, LI Fu-guo. Effect of particle characteristics on deformation of particle reinforced metal matrix composites [J]. *Transactions of Nonferrous Metals Society of China*, 2010, 20(4): 655–661.
- [24] YEROKHIN A L, LYUBIMOV V V, ASHITKOV R V. Phase formation in ceramic coatings during plasma electrolytic oxidation of aluminium alloys [J]. *Ceramics International*, 1998, 24(1): 1–6.
- [25] YEROKHIN A L, NIE X, LEYLAND A, MATTHEWS A. Characterization of oxide films produced by plasma electrolytic oxidation of a Ti–6Al–4V alloy [J]. *Surface and Coatings Technology*, 2000, 130(2–3): 195–206.
- [26] XUE W, DENG Z, CHEN R, ZHANG T, MA H. Microstructure and properties of ceramic coatings produced on 2024 aluminum alloy by microarc oxidation [J]. *Journal of Materials Science*, 2001, 36(11): 2615–2619.
- [27] ZHANG Y, YAN C, WANG F, LOU H, CAO C. Study on the environmentally friendly anodizing of AZ91D magnesium alloy [J]. *Surface and Coatings Technology*, 2002, 161(1): 36–43.
- [28] SONG L W, SONG Y W, SHAN D Y, ZHU GY, HAN E H. Product/metal ratio (PMR): A novel criterion for the evaluation of electrolytes on micro-arc oxidation (MAO) of Mg and its alloys [J]. *Science China: Technological Sciences*, 2011, 54(10): 2795–2801.
- [29] SNIZHKO L O, YEROKHIN A L, PILKINGTON A, GUREVINA N L, MISNYANKIN D O, LEYLAND A, MATTHEWS A. Anodic processes in plasma electrolytic oxidation of aluminium in alkaline solutions [J]. *Electrochimica Acta*, 2004, 49(13): 2085–2095.
- [30] NITIN P W, JYOTHIRMAYI A, KRISHNA L R,

- SUNDARARAJAN G. Effect of micro arc oxidation coatings on corrosion resistance of 6061-Al Alloy [J]. *Journal of Materials Engineering and Performance*, 2008, 17(5): 708–713.
- [31] YAO Z, JIANG Z, XIN S, SUN X, WU X. Electrochemical impedance spectroscopy of ceramic coatings on Ti-6Al-4V by micro-plasma oxidation [J]. *Electrochimica Acta*, 2005, 50(16–17): 3273–3279.
- [32] ARRABAL R, MATYKINA E, HASHIMOTO T, SKELDON P, THOMPSON G E. Characterization of AC PEO coatings on magnesium alloys [J]. *Surface and Coatings Technology*, 2009, 203(16): 2207–2220.
- [33] CIMENOGLU H, GUNYUZ M, KOSE G T, BAYDOGAN M, UGURLU F, SENER C. Micro-arc oxidation of Ti6Al4V and Ti6Al7Nb alloys for biomedical applications [J]. *Materials Characterization*, 2011, 62(3): 304–311.
- [34] MELHEM A, HENRION G, CZERWIEC T, BRIANCON J L, DUCHANOY T, BROCHARD F, BELMONTE T. Changes induced by process parameters in oxide layers grown by the PEO process on Al alloys [J]. *Surface and Coatings Technology*, 2011, 205(2): 133–136.
- [35] NIE X, LEYLAND A, SONG H W, YEROKHIN AL, DOWEY SJ, MATTHEWS A. Thickness effects on the mechanical properties of micro-arc discharge oxide coatings on aluminium alloys [J]. *Surface and Coatings Technology*, 1999, 116–119: 1055–1060.
- [36] TIAN J, LUO Z, QI S, SUN X. Structure and antiwear behavior of micro-arc oxidized coatings on aluminum alloy [J]. *Surface and Coatings Technology*, 2002, 154(1): 1–7.
- [37] SUNDARARAJAN G, KRISHNA L R. Mechanisms underlying the formation of thick alumina coatings through the MAO coating technology [J]. *Surface and Coatings Technology*, 2003, 167(2–3): 269–277.
- [38] POSMYK A. Influence of material properties on the wear of composite coatings [J]. *Wear*, 2003, 254(5–6): 399–407.
- [39] KRISHNA L R., SOMARAJU K R C, SUNDARARAJAN G. The tribological performance of ultra-hard ceramic composite coatings [J]. *Surface and Coatings Technology*, 2003, 163–164: 484–490.
- [40] KRISHNA L R, PURNIMA A S, WASEKAR N P, SUNDARARAJAN G. Kinetics and properties of micro arc oxidation deposited on commercial Al alloys [J]. *Metallurgical and Materials Transactions A*, 2007, 370(38): 370–378.
- [41] LIN X Z, ZHU M H, ZHENG J F, LUO J, MO J L. Fretting wear of micro-arc oxidation coating prepared on Ti6Al4V alloy [J]. *Transactions of Nonferrous Metals Society of China*, 2010, 20(4): 537–546.
- [42] CUI S, HAN J, DU Y, LI W. Corrosion resistance and wear resistance of plasma electrolytic oxidation coatings on metal matrix composites [J]. *Surface and Coatings Technology*, 2007, 201(9–11): 5306–5309.
- [43] LEE J M, KANG S B, HAN J. Dry sliding wear of MAO-coated A356/20 vol.% SiC<sub>p</sub> composites in the temperature range 25–180 °C [J]. *Wear*, 2008, 264(1–2): 75–85.
- [44] ZHOU F, WANG Y, DING H, WANG M, YU M, DAI Z. Friction characteristic of micro-arc oxidative Al<sub>2</sub>O<sub>3</sub> coatings sliding against Si<sub>3</sub>N<sub>4</sub> balls in various environments [J]. *Surface and Coatings Technology*, 2008, 202(16): 3808–3814.
- [45] ZHOU F, WANG Y, LIU F, MENG Y, DAI Z. Friction and wear properties of duplex MAO/CrN coatings sliding against Si<sub>3</sub>N<sub>4</sub> ceramic balls in air water and oil [J]. *Wear*, 2009, 267(9–10): 1581–1588.
- [46] ZHANG P, NIE X, HENRY H, ZHANG J. Preparation and tribological properties of thin oxide coatings on an Al383/SiO<sub>2</sub> metallic matrix composite [J]. *Surface and Coatings Technology*, 2010, 205(6): 1689–1696.

## 微弧氧化处理原位颗粒增强铝基复合材料的磨损性能

Yaman ERARSLAN

Department of Metallurgical and Materials Engineering, Faculty of Chemical and Metallurgical Engineering,  
Yildiz Technical University, Davutpasa Campus, 34210 Esenler, Istanbul, Turkey

**摘要:** 采用微弧氧化工艺来改善原位颗粒增强铝基复合材料的表面性能。通过向铝熔体中加入 15%CuO 来制备 CuAl<sub>2</sub> 增强铝基复合材料。所制备的材料经过热压、均匀化处理、淬火和人工时效处理，然后在含 KOH、KF 和 Na<sub>2</sub>SiO<sub>3</sub> 的电解液中进行微弧氧化处理。经微弧氧化处理，复合材料的表面生成了有效厚度约 15 μm 的 Al<sub>2</sub>O<sub>3</sub> 膜层。洛氏硬度测试后，在压痕边缘部位没有出现裂纹或明显的剥离现象，表明 Al<sub>2</sub>O<sub>3</sub> 膜层与基底结合良好。干摩擦试验结果表明，Al<sub>2</sub>O<sub>3</sub> 膜层对 Al<sub>2</sub>O<sub>3</sub> 球的破坏性作用具有明显的抑制，Al<sub>2</sub>O<sub>3</sub> 膜层的磨损性能比基体提高 15 倍以上。

**关键词:** 原位生成复合材料；铝基复合材料；微弧氧化；磨损；摩擦

(Edited by Sai-qian YUAN)